DEUTSCHES ELEKTRONEN – SYNCHROTRON DESY

DESY 90-148
November 1990

Five Jet Production in Deep Inelastic ep Scattering

A. Dabelstein

II. Institut für Theoretische Physik, Universität Hamburg

ISSN 0418-9833

NOTKESTRASSE 85 · 2 HAMBURG 52

To be sure that your preprints are promptly included in the
HIGH ENERGY PHYSICS INDEX ,
send them to the following address (if possible by air mail) :

DESY
Bibliothek
Notkestrasse 85
2 Hamburg 52
Germany

DESY 90-148
November 1990

ISSN 0418-9833

Five - Jet - Production in Deep Inelastic e P - Scattering

A. Dabelstein
II. Institut für Theoretische Physik, Universität Hamburg

Luruper Chausee 149, D - 2000 Hamburg 50, FRG

Abstract

The five jet cross section of deep inelastic electron - proton scattering is presented. The exact matrix elements in lowest order QCD perturbation theory including neutral currents are calculated. With HERA one can possibly detect these events depending on the resolution cut y_c.

1 Introduction

The physics of multi - jet production in electron - proton- scattering is described by quantum chromodynamics - QCD. We believe that the fundamental particles are the quarks and gluons. The experiments at HERA will start taking data in the near future. Collisions of 30 GeV electrons and 820 GeV protons will be studied. Momentum transfers of $Q^2_{max} = 10^5\ GeV^2$ between electrons and protons are possible. Parton jet events will be observed at the detectors H1 and ZEUS [1]. These rates will be compared with predictions from QCD - perturbation theory.

To get an overview which are the dominant parton processes which contribute to 5 - jet production we have considered first the pure parton processes : production of 4 partons by scattering of a virtual photon or Z boson on an initial quark, antiquark or gluon. Parton masses are neglected throughout and the incomming particles are not polarized. The lepton and hadron tensors are calculated for vector and axial - vector currents. The matrix elements for the various diagrams are known from earlier calculations of 5 - jet production [2]. For e P

scattering we can obtain them from by crossing. We contract the hadron tensor with $g_{\mu\nu}$. This is equivalent to the linear combination $d^2(2\tilde{\sigma}_U - \tilde{\sigma}_L)/dxdy$.

After the partonic cross sections have been worked out we fold them with the known parton distributions to obtain the cross sections for e P $\rightarrow$ e 5 jets. One of the jet is the target remnant jet.

2 Deep Inelastic Cross Section

The reaction

$$e^-(l) + P(p) \rightarrow e^-(l') + p_1 + p_2 + p_3 + p_4 + X \tag{2.1}$$

will be studied. $p_1, ..., p_4$ are the final state partons which are observed as jets. The remnant jet X from the initial proton has momentum p_5. Figure 1 depicts a possible five parton event.

Figure 1:

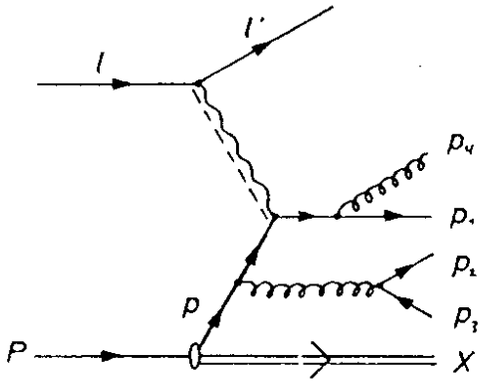

Three and four jet events are discussed in detail in [3]. The hadronic cross section is related to the partonic cross section by :

$$d\sigma_H(P) = \sum_{i=-N_f}^{N_f} \int_0^1 d\eta d\tilde{\sigma}_i(\eta P)\rho_i(\eta) \tag{2.2}$$

where $\rho_i(\eta)$ is the parton distribution function for the parton i (i = 1,...,N_f for quarks, i = 0 for gluon, i= -1,...,$-N_f$ for antiquarks) .
The kinematic variables are denoted as follows :

$$
\begin{aligned}
& q = l - l' && , \quad Q^2 = -q^2 \\
& x = \tfrac{Q^2}{2Pq} && , \quad y = \tfrac{Pq}{Pl} \\
& W^2 = (q+P)^2 = (1-x)ys && \\
& S^2 = (l+P)^2 && , \quad s_p = \eta s \\
& x_p = \tfrac{Q^2}{2pq} && , \quad \eta = \tfrac{x}{x_p}
\end{aligned}
\tag{2.3}
$$

The parton cross section is calculated by :

$$
d\tilde{\sigma}_i^{(A)}(p) = C_i^{(A)}(Q^2)\left(\frac{4\pi\alpha}{Q^2}\right)^2 \frac{1}{2s_p}\frac{d^3l'}{(2\pi)^3 2E'}\; 4\pi\; L_{(A)}^{\mu\nu} W_{\mu\nu}^{(A)} \tag{2.4}
$$

$$
A = \begin{cases} PC & , \; parity\ conserved \\ PV & , \; parity\ violating \end{cases} \tag{2.5}
$$

$C_i^{(A)}$ contains the flavour dependent electroweak coupling constants. These expressions will be given when all classes of diagrams have been discussed.
The lepton and hadron tensor are :

$$
L_{PC}^{\mu\nu} = 2\left(l^\mu l'^\nu + l'^\mu l^\nu - \frac{Q^2}{2} g^{\mu\nu}\right) \tag{2.6}
$$

$$
L_{PV}^{\mu\nu} = 2i\; \epsilon^{\mu\nu\alpha\beta}\; l_\alpha l'_\beta \tag{2.7}
$$

$$
W_{\mu\nu}^{(A),i} = \frac{1}{4\pi}\int dPS^{(4)} H_{\mu\nu}^{(A),i}(p,q,p_1,p_2,p_3,p_4) \tag{2.8}
$$

where $H_{\mu\nu}^{(A),i}$ is the hadron tensor for the initial parton i.
The phase space is :

$$
dPS^{(4)} = \prod_{i=1}^{4} \frac{d^3p_i}{2(2\pi)^3 E_i}\; (2\pi)^4 \delta^4\left(p + q - \sum_{i=1}^{4} p_i\right) \tag{2.9}
$$

Using

$$
\frac{d^3l'}{(2\pi)^3 2E'} = \frac{Q^2}{16\pi^2 x^2 s}\; dx\; dQ^2 \tag{2.10}
$$

we obtain

$$
d\tilde{\sigma}_i^{(A)} = \frac{2\pi\alpha^2}{yQ^2}\; dy\; dx_p \frac{y}{x_p \eta s} L_{(A)}^{\mu\nu} W_{\mu\nu}^{(A),i} \cdot C_i^{(A)} \tag{2.11}
$$

For computational reasons we calculated only the trace of the hadron tensor. This corresponds to the cross section $d(2\tilde{\sigma_U} - \tilde{\sigma}_L)$.

Expressing the parton tensor $W_{\mu\nu}$ by the structure functions F_1^p, F_2^p, F_3^p we get :

$$
W_{\mu\nu}^{PC,i}(p,q) = -\hat{g}_{\mu\nu}\frac{F_1^{P,i}}{2} + \frac{\hat{p}_\mu \hat{p}_\nu}{pq} x_p F_2^{P,i} \tag{2.12}
$$

$$W_{\mu\nu}^{PV,i}(p,q) = \frac{-i}{pq}\epsilon_{\mu\nu\alpha\beta}\ q^\alpha\ q^\beta \frac{F_3^{P,i}}{2} \tag{2.13}$$

The hatted tensors are introduced :

$$\hat{g}_{\mu\nu} = g_{\mu\nu} + \frac{q_\mu q_\nu}{Q^2}$$

$$\hat{p}_\mu = p_\mu + \frac{pq}{Q^2} q_\mu$$

The projection $g^{\mu\nu}W_{\mu\nu}$ is calculated and yields :

$$W_\mu^{\ \mu\ PC}(p,q) = \frac{1}{4\pi}\int dPS^{(4)} g^{\mu\nu} H_{\mu\nu} \tag{2.14}$$

$$W_\mu^{\ \mu\ PV}(p,q) = 0 \tag{2.15}$$

We define the unpolarized $d\tilde{\sigma}_U$ and longitudinal polarized $d\tilde{\sigma}_L$ parton cross section

$$d\tilde{\sigma}_{U,i}^{PC} \equiv C_i^{PC}\frac{2\pi\alpha^2}{yQ^2}\ dy\ dx_p \frac{\epsilon^\mu(1)\epsilon^{\nu *}(1) + \epsilon^\mu(-1)\epsilon^{\nu *}(-1)}{2}\ W_{\mu\nu}^{PC,i} \tag{2.16}$$

$$d\tilde{\sigma}_{L,i}^{PC} \equiv C_i^{PC}\frac{2\pi\alpha^2}{yQ^2}\ dy\ dx_p (\epsilon^\mu(0)\epsilon^{\nu *}(0)) W_{\mu\nu}^{PC,i} \tag{2.17}$$

These definitions give the linear combination :

$$d(2\tilde{\sigma}_U - \tilde{\sigma}_L)_i^{PC} = C_i^{PC}\frac{2\pi\alpha^2}{yQ^2} dy\ dx_p (-g^{\mu\nu}W_{\mu\nu}^i) \tag{2.18}$$

$$= C_i^{PC}\frac{2\pi\alpha^2}{yQ^2} dy\ dx_p (F_2^P - \frac{3}{2}F_L^P)^i \tag{2.19}$$

$$d\tilde{\sigma}_{L,i}^{PC} = C_i^{PC}\frac{1}{2}\frac{2\pi\alpha^2}{yQ^2}\ dy\ dx_p\ F_L^{P,i} \tag{2.20}$$

where $F_L^p \equiv F_2^p - F_1^p$.
Therefore the integrated 5 - jet cross section obtained from the trace of the hadron tensor contributes to the combination of $F_2 - \frac{2}{3}F_L$ of the structure functions. We expect the contribution of the longitudinal part to be small. Thus we obtain from our calculations essentially a contribution to F_2.

3 The Parton Tensor

The hadron tensor H_μ^μ for the deep inelastic scattering can be calculated by applying a crossing symmetry to the hadron tensor in e^+e^- annihilation. The expressions from [2] are used and neutral currents are taken into account. The configurations in the initial and final

states are :

I) initial quark :

$$l + q(p) \to l' + q(p_1) + q(p_2) + \bar{q}(p_3) + G(p_4)$$
$$l + q(p) \to l' + q(p_1) + G(p_2) + G(p_3) + G(p_4)$$
$$l + q(p) \to l' + q(p_1) + ghosts + G(p_4)$$

II) initial antiquark :

$$l + \bar{q}(p) \to l' + \bar{q}(p_1) + q(p_2) + \bar{q}(p_3) + G(p_4)$$
$$l + \bar{q}(p) \to l' + \bar{q}(p_1) + G(p_2) + G(p_3) + G(p_4)$$
$$l + \bar{q}(p) \to l' + \bar{q}(p_1) + ghosts + G(p_4)$$

III) initial gluon :

$$l + G(p) \to l' + q(p_1) + \bar{q}(p_2) + q(p_3) + \bar{q}(p_4)$$
$$l + G(p) \to l' + q(p_1) + \bar{q}(p_2) + G(p_3) + G(p_4)$$
$$l + G(p) \to l' + q(p_1) + \bar{q}(p_2) + ghosts$$

Crossing the $e^+e^- \to 5\ jet$ topologies yields the scattering diagrams.
For example :

Figure 2:

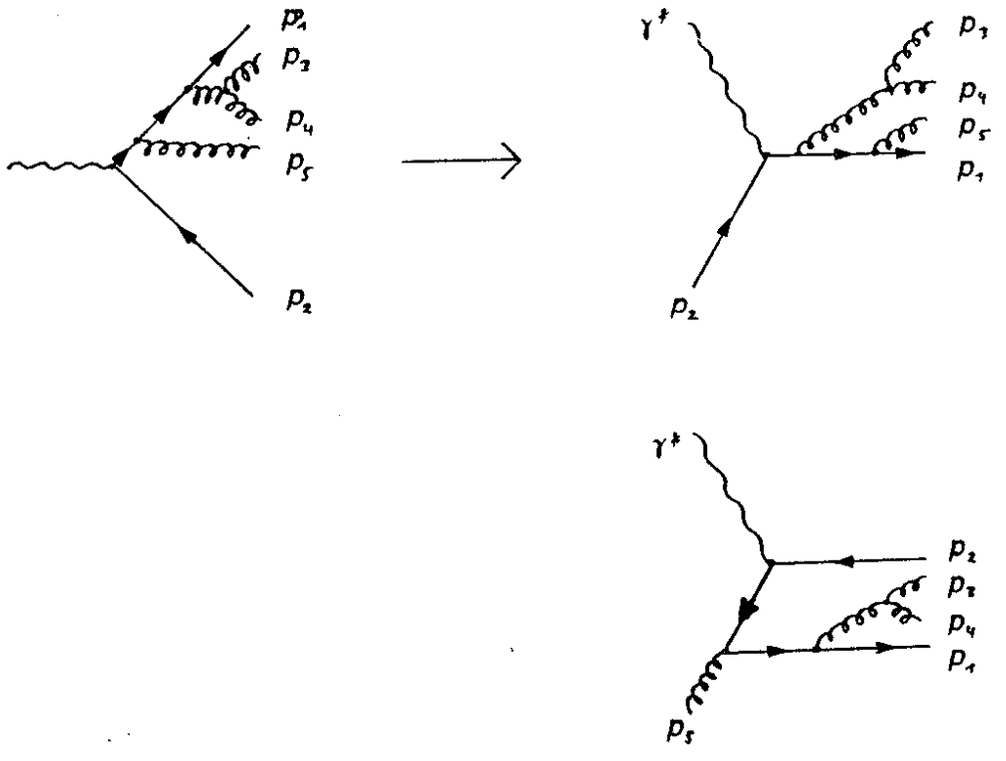

The changes in the hadron tensor for $e^+e^- \to 5$ *jets* are the following :

I) initial quark :

The initial momentum p_2 changes sign. The hadron tensor H_μ^μ gets a multiplicative factor (-1).

II) initial antiquark :

The initial momentum p_1 changes sign. H_μ^μ is multiplied by (-1).

III) initial gluon :

Just the momentum p_5 changes sign.

The topologies are related to different classes. Flavour sums, coupling constants and propagators are given for each class. Parity violating expressions are not relevant.

1) quark / antiquark $\to$ quark / antiquark + 3 gluon

Figure 3:

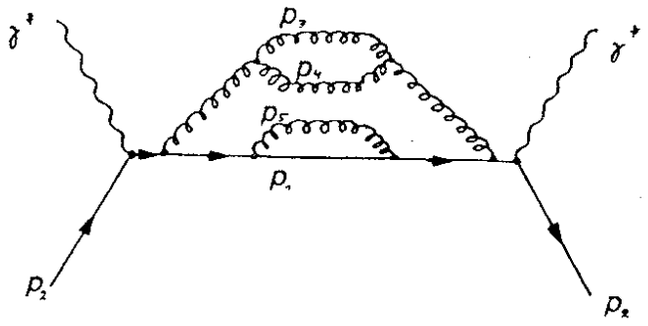

The expressions $C_i^{PC}(Q^2)$ (2.18) are :

$$C_i^{PC}(Q^2) = \frac{1}{2} \cdot \frac{1}{3} \cdot \frac{1}{6} \cdot A_i^{PC}(Q^2) \tag{3.1}$$

where

$$A_i^{PC}(Q^2) = e_i^2 + 2e_i v_i \Re(\chi_Z)(-v_e) + (v_i^2 + a_i^2) \mid \chi_Z \mid^2 (v_e^2 + a_e^2) \tag{3.2}$$

Initial state electrons are not polarized. The first factor $\frac{1}{2}$ arises from initial spin averaging, $\frac{1}{3}$ from quark colour states and $\frac{1}{6}$ from gluon permutation symmetry.
The coupling constants and propagators are :

$$\begin{aligned} e_i &: \quad \textit{quark charge} \\ v_i &= 2t_i - 4e_i \sin^2\theta_W \\ v_e &= -1 + 4\sin^2\theta_W \end{aligned} \tag{3.3}$$

$$\begin{aligned} a_i &= 2t_i \\ a_e &= -1 \end{aligned} \tag{3.4}$$

$$t_i = \begin{cases} 1/2 & for\ u,\ c\ quarks \\ -1/2 & for\ d,\ s,\ b\ quarks \end{cases} \tag{3.5}$$

$$\chi_Z(Q^2) = \frac{1}{(2\sin(2\theta_W))^2} \cdot \frac{Q^2}{Q^2 + M_Z^2 - i\ M_Z\Gamma_Z} \tag{3.6}$$

2) gluon → quark + antiquark + 2 gluon

Figure 4:

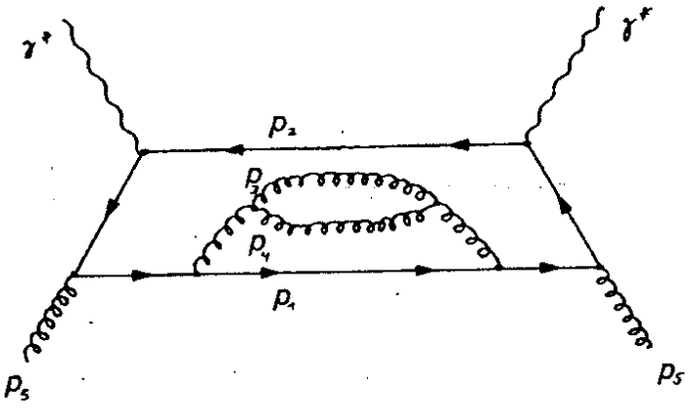

$$C_j^{PC} = \frac{1}{2} \cdot \frac{1}{8} \cdot \frac{1}{2} \cdot A_j^{PC}(Q^2) \tag{3.7}$$

Flavour summing is done. $(j = u, d, s, c, b)$

3) quark / antiquark → quark / antiquark + 2 quark + 1 gluon

Figure 5:

class D :

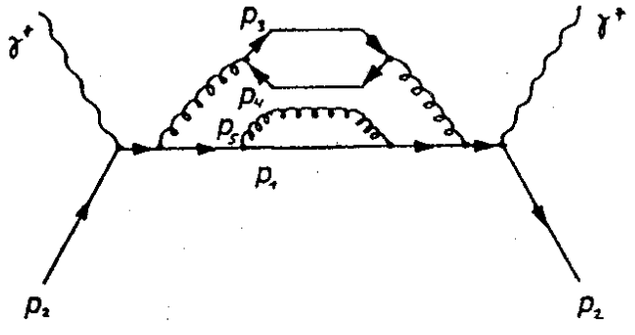

$$C_i^{PC} = \frac{1}{2} \cdot \frac{1}{3} \cdot \frac{1}{2} A_i^{PC}(Q^2) \cdot N_F \quad , N_f = 5 \tag{3.8}$$

Figure 6:

class D' :

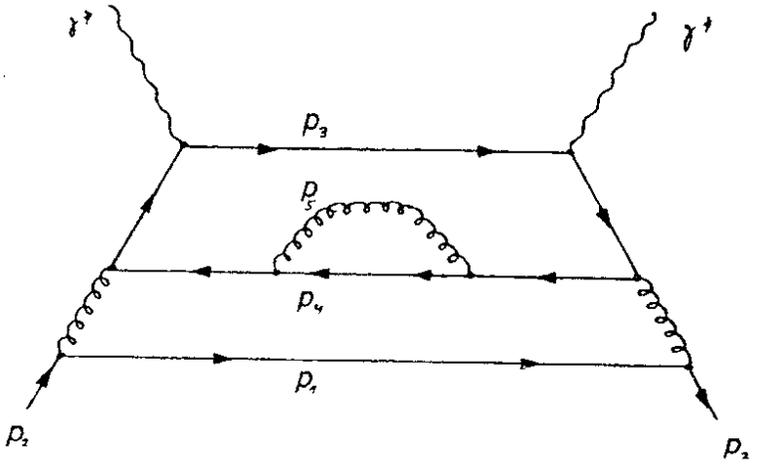

$$C_j^{PC} = \frac{1}{2} \cdot \frac{1}{3} \cdot \frac{1}{2} A_j^{PC}(Q^2) \tag{3.9}$$

Figure 7:

class F :

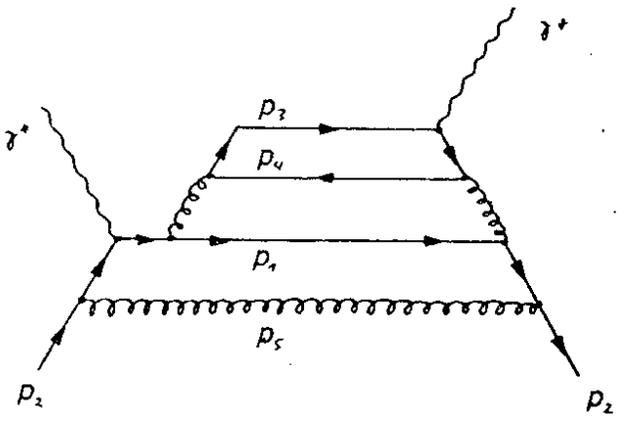

$$C_{i,j}^{VV,AA} = \frac{1}{2} \cdot \frac{1}{3} \cdot \frac{1}{2} A_{i,j}^{VV,AA}(Q^2) \qquad , j = u,\ d, ...,\ b \tag{3.10}$$

with

$$A_{i,j}^{VV}(Q^2) = e_i e_j + (e_i v_j + e_j v_i)\Re(\chi_Z)(-v_e) + v_i v_j \mid \chi_Z \mid^2 (v_e^2 + a_e^2) \tag{3.11}$$

$$A_{i,j}^{AA}(Q^2) = +a_i a_j \mid \chi_Z \mid^2 (v_e^2 + a_e^2) \tag{3.12}$$

The sign of the expression $A_{i,j}^{VV}$ changes when the class is folded with an antiquark distribution function.

Figure 8:

class E :

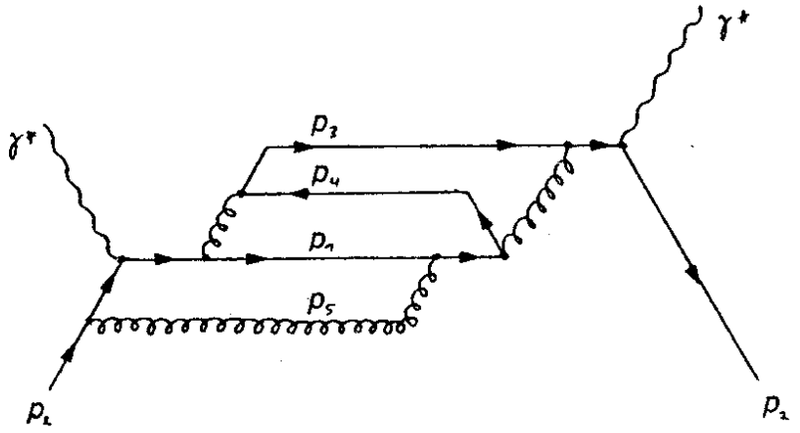

$$C_i^{PC} = \frac{1}{2} \cdot \frac{1}{3} \cdot \frac{1}{2} A_i^{PC}(Q^2) \tag{3.13}$$

and $A_i^{PC}(Q^2)$ from (3.18) .

4) gluon $\rightarrow$ 4 quarks :

Figure 9:

class G :

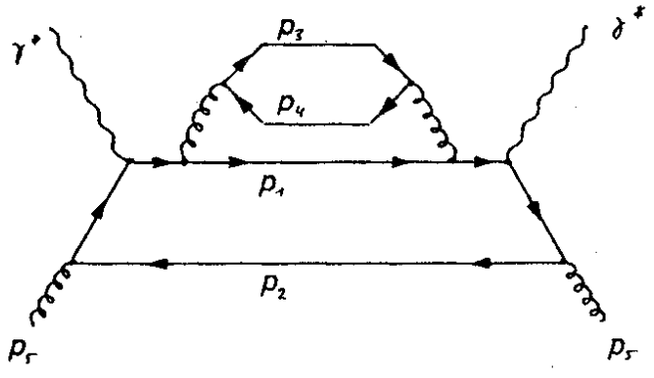

$$C_j^{PC} = \frac{1}{2} \cdot \frac{1}{8} \cdot \frac{1}{4} A_j^{PC}(Q^2) \cdot N_F \tag{3.14}$$

Figure 10:

class H :

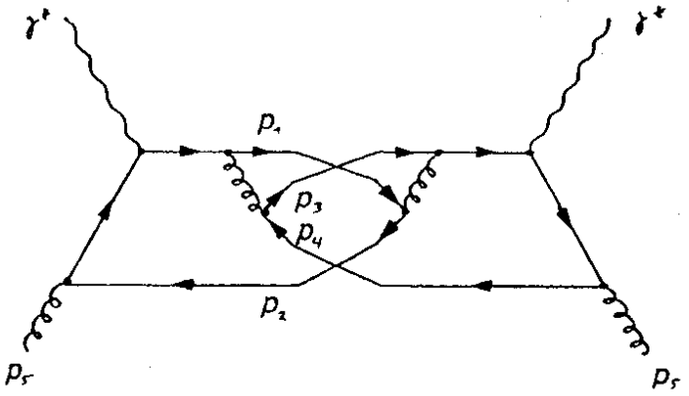

$$C_{i,j}^{VV,AA} = \frac{1}{2} \cdot \frac{1}{8} \cdot \frac{1}{4} A_{i,j}^{VV,AA}(Q^2) \tag{3.15}$$

Figure 11:

class J :

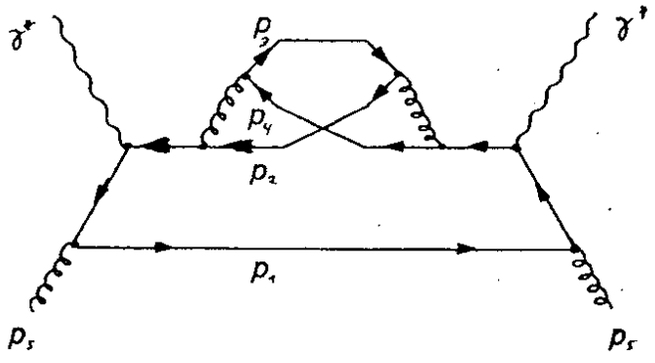

$$C_j^{PC} = \frac{1}{2} \cdot \frac{1}{8} \cdot \frac{1}{4} A_j^{PC}(Q^2) \tag{3.16}$$

4 Numerical Results

The hadron tensor H_μ^μ integrated over the phase space yields the parton tensor by equation (2.8). The integrand contains singularities from collinear or infrared partons.
A resolution cut y_c is defined :

$$s_c \equiv y_c \cdot W_0^2 \quad , \; W_0^2 = (p+q)^2 \tag{4.1}$$

where $s_{i,j} = 2p_i p_j \geq s_c$ forms the boundary condition of the four particle phase space volume.

The parton tensor $W_\mu^\mu(y_c)$ for initial quark is computed for resolution cuts y_c = 0,01 ; 0,02 ; 0,03 and 0,04 . The integration over the four particle phase space was done by using VEGAS [4]. The classes discussed in section 3 are represented separately. The statistical factors N, and the averaging factors from initial colour and spin states are considered. Table 1 gives a general view of the contribution of the various classes to the trace of the hadron tensor. The analogous results for initial gluon scattering are given in table 2. The main contributions of the parton tensor arise from the $Q \to Q3G$ and $G \to 2Q2G$ processes. The $Q \to 3Q1G$ contribution is about 10% thereof. The classes H and J are negligible.

Table 1:

	y_c			
Process	0.01	0.02	0.03	0.04
Q→ Q 3G	0.377	0.123	0.0532	0.0255
Q→ Q ghost 1G	0.00388	0.001433	0.000667	0.000337
Q→ 3Q 1G class D	0.0467	0.0188	0.00927	0.00487
Q→ 3Q 1G class D'	0.00340	0.001286	0.000616	0.000326
Q→ 3Q 1G class F, VV	$-9.85\cdot10^{-6}$	$-4.40\cdot10^{-6}$	$-2.95\cdot10^{-6}$	$-1.34\cdot10^{-6}$
Q→ 3Q 1G class F, AA	$-42.7\cdot10^{-6}$	$-25.8\cdot10^{-6}$	$-16.41\cdot10^{-6}$	$-10.3\cdot10^{-6}$
Q→ 3Q 1G class E	0.000910	0.000413	0.000225	0.000130

The $G \rightarrow 4Q$ contributions are even smaller. Only the classes D and D' give the main contributions to the parton tensor for $Q \rightarrow 3Q1G$.

The parton cross section $d^2(2\tilde{\sigma_U} - \tilde{\sigma_L})/dxdy$ is evaluated for $\sqrt{s} = 314$ GeV at the point x = 0.4 , $Q^2 = 2.2 \cdot 10^4\ GeV^2$ ($\alpha = 1/137$ and $\alpha_s = 0.2$) . The cross section is represented in table 3 for the discussed processes and plotted in figure 12 . The initial quark is an up - quark. For large y_c values the parton cross section decreases as expected. The processes $Q \rightarrow Q3G$ and $G \rightarrow 2Q2G$ give the main contributions. The processes $Q \rightarrow 3QG$ contribute by a factor of 10 and $G \rightarrow 4Q$ are down by factor of ≈ 100.

From this table it can be seen that in order to get an estimate of the 5 - parton cross section a restriction to the processes $Q \rightarrow 3QG$ and $G \rightarrow 2Q2G$ is sufficient.

Table 2:

	y_c			
Process	0.01	0.02	0.03	0.04
G→ 2Q 2G	0.127	0.0367	0.0153	0.00725
G→ 2Q ghost	0.00491	0.00175	0.000688	0.000328
G→ 4Q class G	0.00312	0.00115	0.000534	0.000270
G→ 4Q class H, VV	$1.29 \cdot 10^{-6}$	$0.806 \cdot 10^{-6}$	$0.507 \cdot 10^{-6}$	$0.316 \cdot 10^{-6}$
G→ 4Q class H, AA	$-3.84 \cdot 10^{-6}$	$-2.21 \cdot 10^{-6}$	$-0.838 \cdot 10^{-6}$	$-0.828 \cdot 10^{-6}$
G→ 4Q class J	$-1.84 \cdot 10^{-6}$	$-1.14 \cdot 10^{-6}$	$-0.688 \cdot 10^{-6}$	$-0.444 \cdot 10^{-6}$

By folding the parton cross section with the chosen parameterisation of the EMC - data [5,6] the 5 - jet cross section on protons is obtained. The strong coupling constant α_s is taken in next to leading order [7] where the number of flavours $N_f = 5$ and $\Lambda_{\bar{MS}} = 100 MeV$.

The flavour sum yields :

$$\frac{d^2(2\sigma_U - \sigma_L)_{5jet}}{dy\ dx} = \sum_{i=-N_f}^{N_f} \int_x^1 \frac{dx_p}{x_p} \frac{d^2(2\tilde{\sigma}_U - \tilde{\sigma}_L)(\frac{x}{x_p})}{dy\ dx_P} \cdot \rho(\frac{x}{x_p}) \qquad (4.2)$$

The additional integration was done by VEGAS.

Table 3:

$$\frac{d^2(2\tilde{\sigma}_U - \tilde{\sigma}_L)}{dydx_p}\ [pb]$$

y_c	Q → Q 3G	Q → 3Q G	Q → 5 Jet	G → 2Q 2G	G → 4Q	G → 5 Jet
0.01	$0.295{\cdot}10^{-3}$	$0.0464{\cdot}10^{-3}$	$0.342{\cdot}10^{-3}$	$0.312{\cdot}10^{-3}$	$0.000798{\cdot}10^{-3}$	$0.320{\cdot}10^{-3}$
0.02	$0.0960{\cdot}10^{-3}$	$0.0186{\cdot}10^{-3}$	$0.115{\cdot}10^{-3}$	$0.0890{\cdot}10^{-3}$	$0.000294{\cdot}10^{-3}$	$0.0929{\cdot}10^{-3}$
0.03	$0.0416{\cdot}10^{-3}$	$0.00911{\cdot}10^{-3}$	$0.0507{\cdot}10^{-3}$	$0.0374{\cdot}10^{-3}$	$0.000137{\cdot}10^{-3}$	$0.0387{\cdot}10^{-3}$
0.04	$0.0199{\cdot}10^{-3}$	$0.00480{\cdot}10^{-3}$	$0.0248{\cdot}10^{-3}$	$0.0178{\cdot}10^{-3}$	$0.000069{\cdot}10^{-3}$	$0.0185{\cdot}10^{-3}$

Table 4:

$$R_5(y_c)$$

y_c	Q → Q 3G	Q → 3Q G	G → 2Q 2G	G → 4Q	$e^- P \rightarrow$ 5 Jet
0.01	0.00755	0.00135	0.000646	0.0000235	0.00956
0.02	0.000647	0.000150	0.0000457	0.00000223	0.000845
0.03	0.0000609	0.0000144	$3.18{\cdot}10^{-6}$	$0.219{\cdot}10^{-6}$	0.0000786
0.04	0.000012	$1.1{\cdot}10^{-6}$	$0.38{\cdot}10^{-6}$	$0.015{\cdot}10^{-6}$	0.000013

The ratio $R_5(y_c, Q^2, x)$ is defined :

$$R_5(y_c, Q^2, x) = \frac{d^2(2\sigma_U - \sigma_L)_{5jet}}{dxdy} \Big/ \frac{d^2\sigma_2}{dxdy} \tag{4.3}$$

$$\frac{d^2\sigma_2}{dxdy} = \frac{2\pi\alpha^2}{yQ^2}(1 + (1-y)^2) \cdot F_2$$

where F_2 is the usual structure function from [6] that describes the total inclusive e P cross section evaluated at same Q^2 and x. Table 4 presents the ratio for x = 0.4 , $Q^2 = 50\ GeV^2$ and $W^2 = 75\ GeV^2$ which is plotted in Fig. 13 .

The $Q \rightarrow Q3G$ and $Q \rightarrow 3QG$ processes give the main contributions to the ratio R_5 .

The parton cross section gives contributions to the integrand of equation (4.2) in case of :

$$\eta \geq 6y_c + x\ (1 - 6y_c)\ in\ O(\alpha_s^3) \tag{4.4}$$

If we take y_c and x as fixed parameters the 5 - jet cross section decreases with larger Q^2 - values. For that reason we have chosen $Q^2 = 50\ GeV^2$.

The five jet cross section for fixed y_c and Q^2 parameters increases when x goes to smaller values. We mention that the ratio $R_5(y_c, Q^2, x)$ behaves in a different way. If y_c and Q^2 are fixed R_5 decreases with smaller x values.

These phenomena can be compared with the ratio R_3 of 3 - jet events over the total $O(\alpha_s)$ cross section [3] which show the same x dependence for fixed Q^2 and y_c.

5 Summary

Deep inelastic e^-P scattering in 5 jets was considered. A resolution cut y_c was introduced and the cross section $d^2(2\sigma_U - \sigma_L)/dxdy$ was computed numerically for fixed x = 0.4 , $Q^2 = 50\ GeV^2$. Values for different parameters x, Q^2 and y_c can be computed easily but consume a large amount of CPU time.

5.1 Acknowledgements

I would like to thank Prof. G. Kramer for suggesting the problem and D. Graudenz for fruitful discussions.

Figure 12:

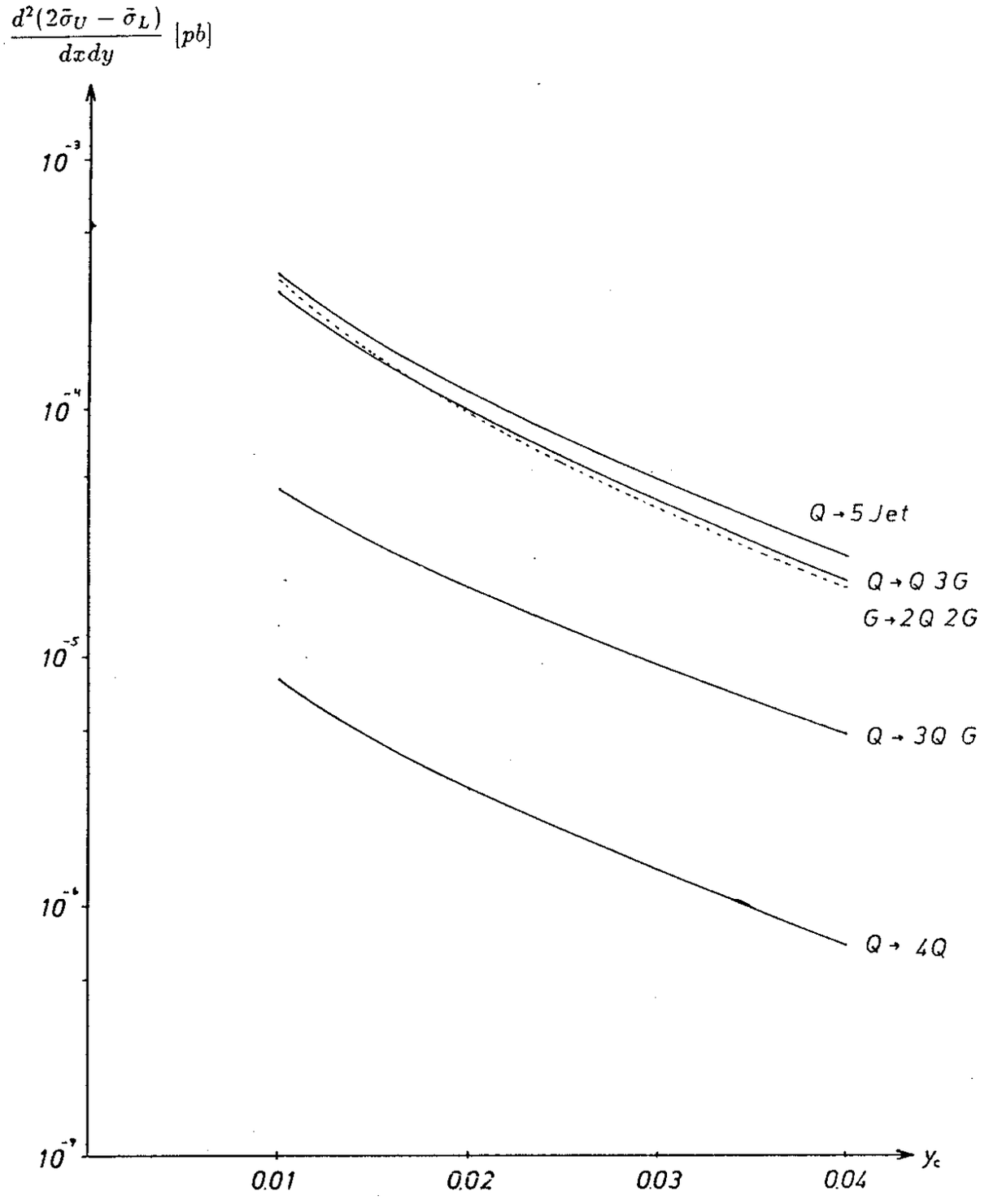
$\frac{d^2(2\bar{\sigma}_U - \bar{\sigma}_L)}{dxdy}$ [pb]
10^{-3}
10^{-4}
10^{-5}
10^{-6}
10^{-7}
0.01
0.02
0.03
0.04
y_c
Q → 5 Jet
Q → Q 3G
G → 2Q 2G
Q → 3Q G
Q → 4Q

Figure 13:

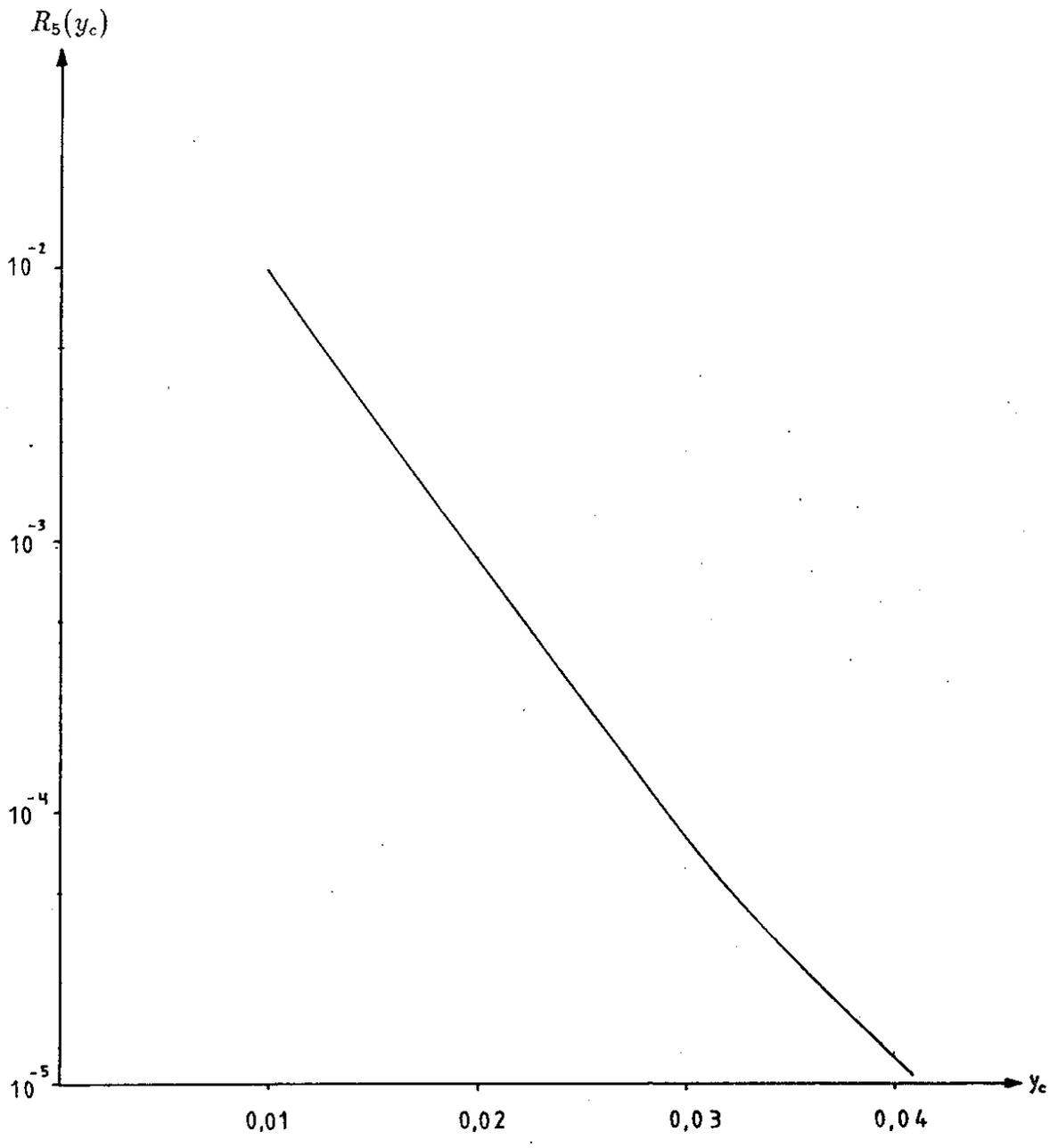

References

[1] ECFA - report 80-42, DESY - HERA 80-01

G. Wolf, DESY - report 86-089

[2] N.N. Falck, D. Graudenz und G. Kramer, Phys. Lett. **B 220** (1989) 299

N.N. Falck, D. Graudenz und G. Kramer, Nucl. Phys. **B 328** (1989) 317

N.N. Falck, D. Graudenz und G. Kramer, Comp. Phys. Comm. **56** (1989) 181

[3] J.G. Körner, E. Mirkes und G.A.Schuler, Int.J. Mod. Phys. **A 4** (1989) 1781

T. Brodkorb, J.G. Körner, E. Mirkes und G.A. Schuler, Z. Phys. **C 44** (1989) 415

[4] S. de Jong und J. Vermaseren, "AXO USER Manual", NIKHEF-H , Amsterdam (1987)

[5] D.N. Harriman, A.D. Martin, W.J. Stirling und R.G. Roberts, RAL-90-007

[6] J.J. Aubert et al., Nucl. Phys. **B259** (1985) 189

J.J. Aubert et al., Nucl. Phys. **B293** (1987) 740

M. Arneodo et al., preprint CERN-EP/89-121

[7] Particle Data Group, Phys. Lett. **B 204** (1988)